An Empiric Correlation of Some Transonic Aerofoil Characteristics

J. C. GIBBINGS*
University of Liverpool, Liverpool, England

For symmetrical aerofoils at zero incidence in transonic flows, use of a nozzle analogy led to good correlations for the critical Mach number, the stock wave position, the crest Mach number, and the slope of the Mach number distribution at the crest. The independent variables used were the stream Mach number, the aerofoil curvature at the crest, the chordwise crest position, and the aerofoil thickness. The latter is only important at the lower end of the transonic speed range.

Nomenclature

a^x = velocity of sound at sonic speed
c = aerofoil chord
h^x = nozzle height at the throat, sonic conditions
h_{cr} = nozzle height corresponding to $M_0 = M_{cr}$
h_0 = nozzle height corresponding to M_0
h_s = nozzle height corresponding to shock position
h_T = nozzle height at the throat
$\bar{M}$ = mean throat Mach number
M_{crest} = Mach number at the aerofoil crest
$M_{crest}{}^x$ = $\equiv q/a^x$
M_{cr} = stream Mach number for sonic speed at the aerofoil crest
M_0 = stream Mach number
R = radius of curvature of the aerofoil surface at its crest
t = aerofoil thickness
x, y = aerofoil ordinates
$X \equiv \dfrac{(h_0/h^x) - 1}{(R/c)(1 - 0.025\,c/t)[(h_{cr}/h^x) - 1]}$
$Y \equiv \dfrac{h_s/h^x - 1}{(R/c)(1 - 0.025\,c/t)[(h_{cr}/h^x) - 1]}$
x_{crest} = coordinate of aerofoil crest
δ^* = boundary-layer displacement thickness at the crest

1. Introduction

TAYLOR, in investigating the flow at the crest of an aerofoil at subcritical speeds, employed a model of the flow in which the upper surface of the aerofoil formed the throat of a nozzle.[1] An outer streamline was assumed straight to represent the nozzle centerline.

This model is used here to aid correlation of experimental results obtained for various aerofoil characteristics in the transonic speed range. It is adopted on two counts. First, it is known that the aerodynamic characteristics at the throat of a nozzle are affected strongly by the radius of curvature of the nozzle wall, and thus a simple correlation of characteristics at the crest of an aerofoil might have the aerofoil crest radius of curvature as a strong independent variable. Second, the nozzle concept of ratio of area at the shock position to throat area is used here in correlating the results for the movement of the shock wave along an aerofoil.

This initial study was limited to consideration of symmetrical aerofoils at zero incidence. All the experimental results used were obtained in the slotted-wall, transonic wind tunnels of the Aerodynamics Division, National Physical Laboratory. Three slot-to-wall area ratios were used as detailed in Table 1. The results given in Ref. 2 suggest that there was negligible variation of blockage in using these three area ratios, although they gave differences in their distortion of the sonic line. Variation of slot area ratio was found to have a slight effect upon one of the characteristics considered here. On all models, the boundary layer was tripped to turbulence by a narrow band of roughness at the leading edge. The data was obtained at Reynolds numbers which were the same weak function of Mach number for all the aerofoils: at sonic stream speed, the chord Reynolds number was $1.9.10^6$. A discussion of the significance to the present results of both blockage and viscous effects is given later.

Received August 19, 1965; revision received February 28, 1966. The author is indebted to many of the staff of the Aerodynamics Division, National Physical Laboratory, for their ready assistance which enabled him to carry out the work described herein. In particular, he is grateful to E. W. E. Rogers and C. S. Sinnott for help in collecting available data, and to H. H. Pearcey for additionally drawing attention to relevant existing work.

* Ph.D., Fluid Mechanics Division, Department of Mechanical Engineering.

2. Correlation of Experimental Results

2.1 Critical Stream Mach Number

The aerofoil critical Mach number is taken as that free-stream Mach number for which sonic speed occurs at the aerofoil maximum thickness point. This latter position here is referred to as the aerofoil crest. With some aerofoils, local sonic speed first is attained away from the crest at a lower stream Mach number than this critical; this is particularly so with the NPL 491 aerofoil which had a noticeable peak in the velocity distribution well upstream of the crest. No account

Table 1 Code to diagram symbols

Aerofoil	Symbol	Remarks
4% Biconvex	⊙	Slotted working section of 1/11th area ratio
4% R.A.E. 104	▽	Slotted working section of 1/8th area ratio
	▽	Slotted working section of 1/30th area ratio
4% N.P.L. 491	△	Slotted working section of 1/11th area ratio
6% R.A.E. 104	◹	Upper surface — Incidence of −0.3°
	◸	Lower surface — Incidence of −0.3°
	◹	Mean of upper and lower surface values — Slotted working section of 1/30th area ratio
6% R.A.E. 102	⊡	Slotted working section of 1/8th area ratio
	⊡	Slotted working section of 1/30th area ratio
N.A.C.A. 00095	×	Upper surface — Slotted working section of 1/30th area ratio
	+	Lower surface — Slotted working section of 1/30th area ratio
10% R.A.E. 104	◇	Slotted working section of 1/11th area ratio
10% R.A.E. 102	⌓	Slotted working section of 1/30th area ratio

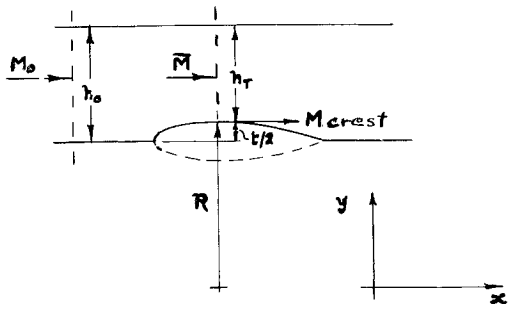

Fig. 1 Sketch of nozzle flow model.

has been taken of this effect, since all values analyzed were crest ones.

Adopting the corresponding nozzle flow as a model for the aerofoil flow, we have on the basis of one-dimensional isentropic channel flow (as sketched in Fig. 1) that the mean throat Mach number $\bar{M}$ can be written

$$\bar{M} = f(M_0, h_0/h_T) \tag{1}$$

For the two-dimensional flow at the nozzle throat, we also can write (see, for instance, Ref. 3),

$$\bar{M}/M_{\text{crest}} = f(h_T, (d^2y/dx^2), (d^3y/dx^3) \ldots) \tag{2}$$

where x and y are the nozzle ordinates. Retaining only first-order terms, then Eq. (2) just becomes

$$\bar{M}/M_{\text{crest}} = f[h_T \cdot (d^2y/dx^2)] \tag{3}$$

Now with nose-to-tail reversal of a symmetrical aerofoil at zero incidence, either in isentropic flow or in a real flow with a thin boundary layer, there is no change in M_{crest}.[4] There is, however, a change in sign of d^2y/dx^2; and so it is convenient to replace this quantity by the radius of curvature at the crest R which is regarded always as positive.

Thus, Eq. (3) can be written

$$\bar{M}/M_{\text{crest}} = f(R/h_T) \tag{4}$$

Additionally, from the nozzle shape, we have

$$h_0 - h_T = t/2 \tag{5}$$

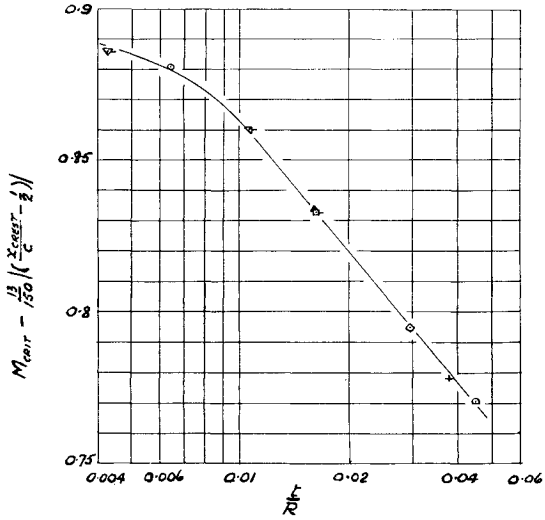

Fig. 2 Correlation of critical Mach number as a function of thickness—radius ratio (symbol code in Table 1).

Eliminating $\bar{M}$ and h_T from Eqs. (1, 4, and 5) reduces them to a single relation of the form,

$$M_0 = f(M_{\text{crest}}, R, t, h_0)$$

Expecting that, of the last three independent variables, R and t would be the most significant, then the nondimensional products are arranged in the form,

$$M_0 = f(M_{\text{crest}}, R/t, h_0/t)$$

In plotting the experimental results, the first two independent variables, M_{crest} and R/t, were found to be of significance; but there was no evidence of lack of correlation because of neglect of the third variable h_0/t. Thus, the foregoing relation can be reduced

$$M_0 = f(M_{\text{crest}}, R/t)$$

In the special case when $M_{\text{crest}} = 1.0$ and the corresponding critical value of M_0 is M_{cr} say, then

$$M_{\text{cr}} = f(R/t)$$

When the experimental results were plotted on this basis, there appeared evidence of a significant higher order term, that is, a term involving d^3y/dx^3 at the crest. For most aerofoils this term, which is indicative of the rate of change of curvature at the crest, might be expected to be related roughly to the crest chordwise position, x_{crest}. With nose-to-tail reversal of an aerofoil there is no change in d^3y/dx^3 and if, as before, there is to be no effect upon the value of M_{cr}, then a suitable variable is $|x_{\text{crest}}/c - \frac{1}{2}|$.

The correlation obtained is shown in Fig. 2. It is seen to be quite good for a large range of aerofoils, since the maximum scatter in M_{cr} is about 0.0015.†

2.2 Chordwise Shock Wave Position

The onset and rearward movement of a shock wave on an aerofoil at transonic speeds is very similar in nature to the case of transonic nozzle flow.[5] Thus, the aerofoil flow is represented again by a nozzle flow model which this time is taken to be a choked one-dimensional flow. The shock wave position thus can be represented by the equivalent ratio of cross-sectional area at the shock to that at the nozzle throat. This flow model is sketched in Fig. 3. Also, M_0 can be replaced as a variable by h_0/h^x so that the variable h_s/h^x, which denotes the shock position, can be related to the corresponding aerofoil y ordinate by

$$\frac{h_s}{h^x} - 1 = \left(\frac{h_0}{h^x} - 1\right)\left(1 - \frac{y}{t/2}\right)$$

Values of $(h_s/h^x) - 1$ are plotted against corresponding values of $(h_0/h^x) - 1$ in Fig. 4 using the experimental results for a range of aerofoils. The right-hand sides of these curves correspond to the initial appearance of the aerofoil shock

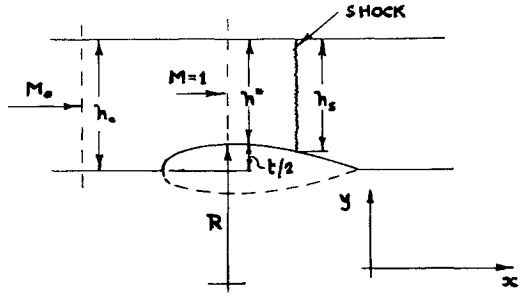

Fig. 3 Sketch of choked nozzle flow model.

† For a family of aerofoils varying only in thickness, $t/R \propto (t/c)^2$.

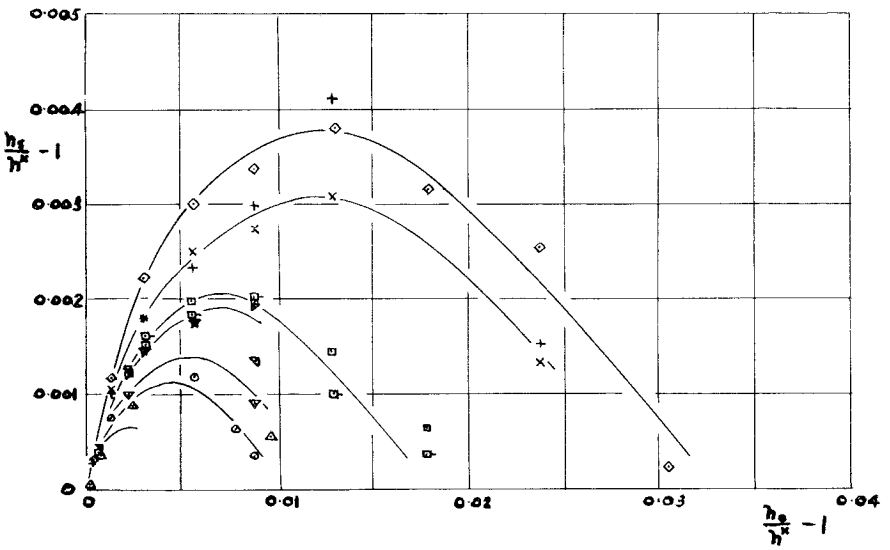

Fig. 4 Area ratio plots for shock wave position (symbol code in Table 1).

wave; the backward movement of the shock with increasing stream Mach number corresponds to movement along these curves toward the origin; and the origin corresponds to a sonic stream.

A further plot, on log scales as in Fig. 5, of the values of $(h_s/h^x) - 1$ and $(h_0/h^x) - 1$ shows that a family of matched curves is obtained with a relative displacement at 45°. Thus, this family of curves has a scaling factor that is the same along both axes.

The smoothed curves of Fig. 4 are replotted in Fig. 6 as solid lines together with values corresponding to the critical Mach number which are plotted as values of $(h_{cr}/h^x) - 1$. The curves for the various aerofoils show no obvious inclination to tend toward their appropriate value of $(h_{cr}/h^x) - 1$. This point is discussed further in the next section, where the dotted lines are also considered. However, h_{cr} appears to be a significant variable in the factor scaling the various curves.

The correction to $(h_{cr}/h^x) - 1$ as a scaling factor was found to be a function of both R/c and t/c. A fair correlation was obtained using the factor

$$(R/c)[1 - 0.025(c/t)][(h_{cr}/h^x) - 1]$$

as shown in the plot of the experimental values in Fig. 7. This factor was obtained independently for the scaling ratios along each axis; but even so, the amount of data used was rather limited.

Although, as pointed out in Sec. 1, the Reynolds number did not differ between the data for the different aerofoils, the variations of their pressure distributions might have an effect upon the growth of the boundary layer downstream of the crest. In this region, the Mach number (as it is close to unity) is very sensitive to the cross-sectional area between streamlines, as indicated by $(h_s - h^x)$. Thus, small variations in this growth between different aerofoil shapes might well explain the scatter to the right-hand end of the curve in Fig. 7 which corresponds to shock wave positions just downstream of the crest.

The effect of different blockages obtained by two area ratios of slotted wall wind tunnel are shown for the 6% Royal Aircraft Establishment (RAE) 102 aerofoil. This blockage difference is seen to be greater when the shock is just downstream of the crest, although there is an inconsistency in the sign of the difference.

To indicate the significance of the amount of scatter about the mean curve of Fig. 7 in terms of shock position, the smoothed curve shown was used to compute this shock position x_{shock}, as a function of M_0 for three aerofoils. The results of these calculations are shown as solid line curves in Fig. 8 together with the experimental values for comparison. The aerofoils chosen cover a range of 4 to 9.5% in thickness chord ratio and a range of 0.3 to 0.5 in values of x_{crest}/c. The error in predicting x_{shock}/c is seen to be small, the maximum error of about 0.04 occurring just downstream of the crest.

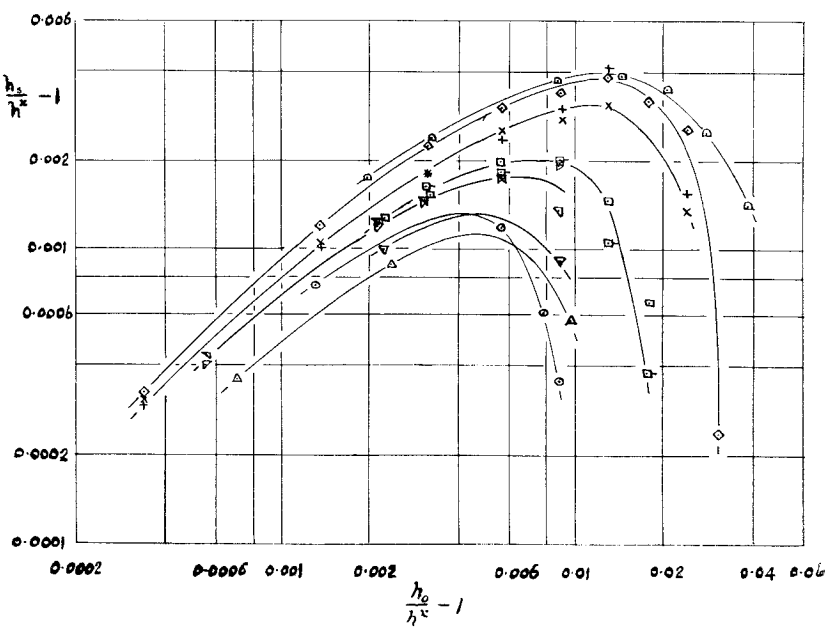

Fig. 5 Replot of Fig. 4 using logarithmic scales.

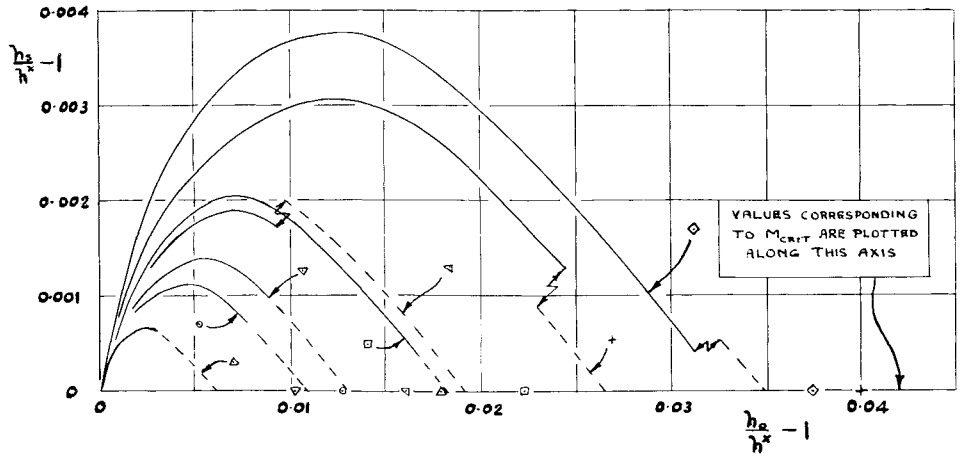

Fig. 6 Replot of the smoothed curves of Fig. 4; dotted lines are reproductions of the mean curve of Fig. 7.

2.3 Onset of a Shock Wave for $M_0 > M_{cr}$

Consider the consequences of assuming both that a single mean curve can be drawn over the whole experimental range of Fig. 7 and that it can be extrapolated as shown dotted, to the point ($X = 0.362$, $Y = 0$). Even if incorrect, the first assumption is not unreasonable if the scatter is attributed to boundary-layer effects. As already pointed out, the value of $X = 0.362$ does not correspond to that value of X that is appropriate to M_{cr}. This point is illustrated in Fig. 6 where the dotted extrapolation of the individual curves is obtained from the single curve of Fig. 7. It is seen that the $Y = 0$ values are in two cases higher than the appropriate critical values, and in the other cases are lower; also, on the basis of the present correlation, no single curve can be drawn in Fig. 7 that will extrapolate to all the appropriate M_{cr} values. But if a shock first appears at the critical stream Mach number, then the curve for each aerofoil in Fig. 6 should end at its appropriate value of $(h_{cr}/h^x) - 1$.

Then, should the single curve fan out at its right-hand end to a series of curves tending to the M_{cr} values? Or should the connection be by a number of discontinuous jumps in either X or Y directions as appropriate? The insufficiency of the present data prohibits a definite answer a point appreciated by comparison of the critical values with the experimental shock positions as marked in Fig. 8. Certainly, if the curve does fan out, then, from the present amount of data for some of those aerofoils with critical values corresponding to $X > 0.362$, these connection curves are near to a discontinuity. This means that for these aerofoils, either there is a delay in the formation of a shock until after the stream Mach number reaches the critical; or if the shock first appears at the critical Mach number, its initial backward movement is very slow. There is some support for the former possibility from the experiments described in Ref. 6.

Those two aerofoils having critical values of X less than 0.362 could have hardly any X values greater than their critical ones, for that would imply shocks appearing before the critical Mach number.‡ Thus, the curves for these two aerofoils would (in Fig. 6) at least drop quite sharply to their critical values. This implies that if the shocks appear at the crest at the critical Mach number, then they have a rapid initial rearward movement.

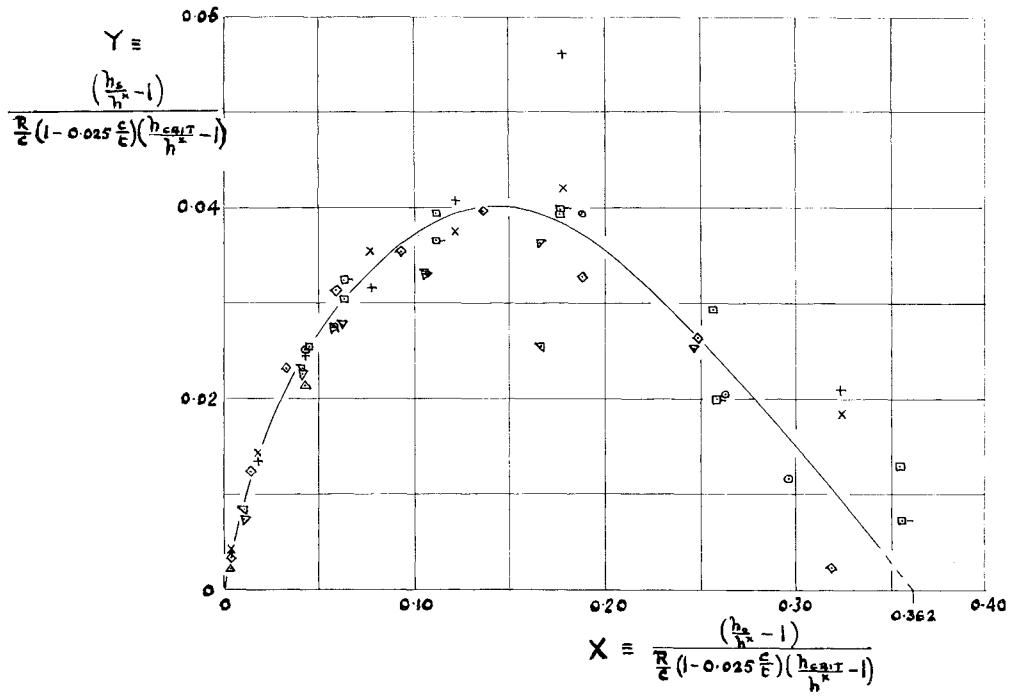

Fig. 7 Correlation of experimental results for variation of shock wave position with stream Mach number (symbol code in Table 1).

‡ These two aerofoils, 4% RAE 104 and 6% RAE 104, each had an almost flat top to their velocity distributions. The subsonic velocity peak on the former occurred at the crest, and on the latter occurred very slightly downstream of the crest. Thus, even though M_{cr} is related here to crest Mach number and not to peak Mach number, this statement still is valid for these two aerofoils.

The dividing line between the two cases of rapid and slow initial shock movement corresponds to $X = 0.362$ and $M_0 = M_{cr}$. This gives the relation

$$\frac{R}{c} = \frac{2.76}{[1 - 0.025(c/t)]} \tag{6}$$

which is plotted in Fig. 9. To this figure are added the values for the aerofoils analysed here.§

2.4 Crest Mach Number—Sonic Stream

After the formation of a shock wave, more and more of the surface flow becomes supersonic with rising stream Mach number until at a sonic stream speed most of it is supersonic. The flowfield thus is approaching a purely supersonic one where linearized theory says that the local aerofoil Mach number is dictated by the aerofoil slope there. Thus, as the stream Mach number rises through the rising transonic speed range, the Mach number at the crest would be expected to become increasingly less dependent upon the thickness as a shape parameter. This was found to be so in the correlation of M_{crest} at $M_0 = 1.0$ as shown in Fig. 10 where R appears to be the prime variable.

The results in Fig. 10 have attached to them the corresponding values of the area ratio of the slotted working section. These suggest that, at this sonic speed, the crest Mach number, as well as being a function of the aerofoil shape, also is sensitive to the variation of this area ratio.¶ Two dotted lines are drawn tentatively in this figure: one for an area ratio of $\frac{1}{8}$th, and the other for the area ratios of

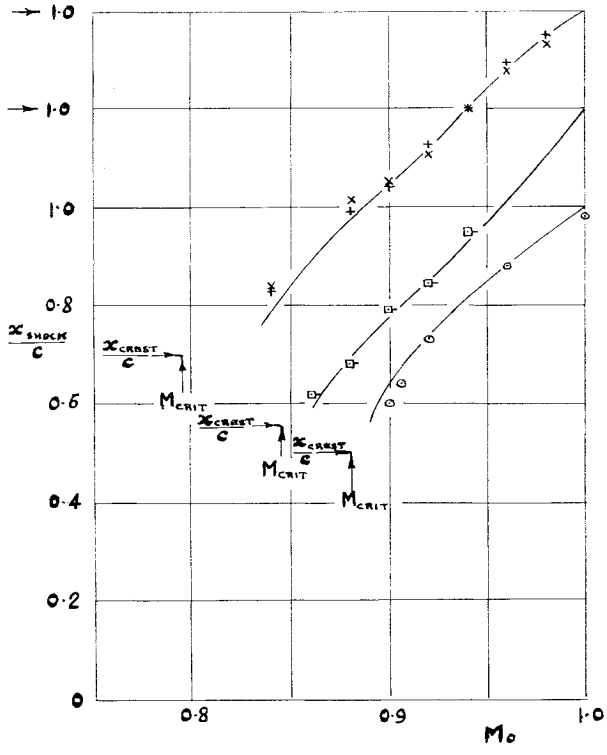

Fig. 8 Examples of use of present method for computing shock wave position. Points are experimental values; solid lines indicate calculated values using the mean curve of Fig. 7 (symbol code in Table 1).

§ A family of identical aerofoils varying only in thickness will appear as a straight line through the origin on this graph. Two examples are shown by dotted lines.

¶ Results for the 6% RAE 102 aerofoil in a working section of $\frac{1}{30}$ area ratio were only available for Mach numbers up to 0.94. At this Mach number, the crest Mach number was lower by 0.01 than for the aerofoil in the $\frac{1}{8}$ area ratio working section.

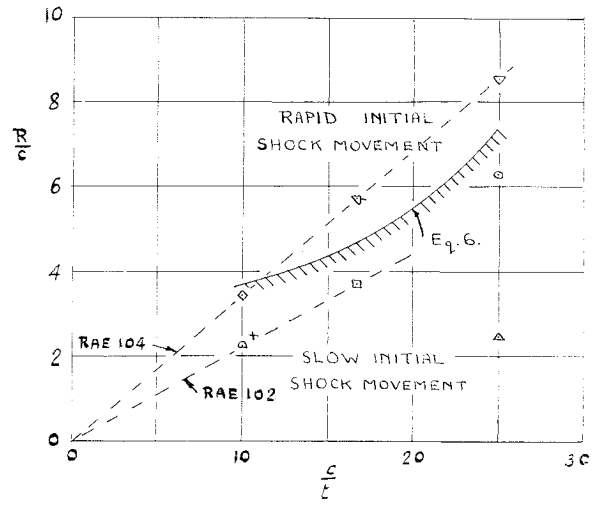

Fig. 9 Boundary between regions of rapid and slow initial shock movement (symbol code in Table 1).

$\frac{1}{11}$th and $\frac{1}{30}$th. The only aerofoil result that does not support this suggestion is that for the NACA 00095. The experimental results for this aerofoil at this speed were unsatisfactory as is evidenced by the results described later in Sec. 2.6.

The maximum error about the mean curve shown solid in Fig. 10, and which fits the relation,

$$M_{crest} - 1 = 0.35(c/R)^{0.53}$$

is ± 2.5%.**

2.5 Variation of Crest Mach Number between Stream Critical and Sonic Speeds

The linearised equations for nozzle flow have been solved using a series solution.[7] The first term of a series for the wall Mach number at the nozzle throat in choked flow gives

$$(M_{crest}{}^2 - 1) = \tfrac{1}{3}(h^2/R)$$

This can be converted readily to

$$(M_{crest} - 1) = 0.4(h^2/R) \tag{7}$$

where also

$$\frac{h^x}{R} = \frac{1}{2R/t[(h_0/h^x) - 1]}$$

Using this as a basis of correlating the aerofoil results, the latter are shown plotted in Fig. 11. The values plot as a family of curves and suggest two flow regimes. The one, represented by the right-hand side of the figure, corresponds to the so called "Mach number freeze" at sonic speeds[8]; the other corresponds to the initial regime just after first

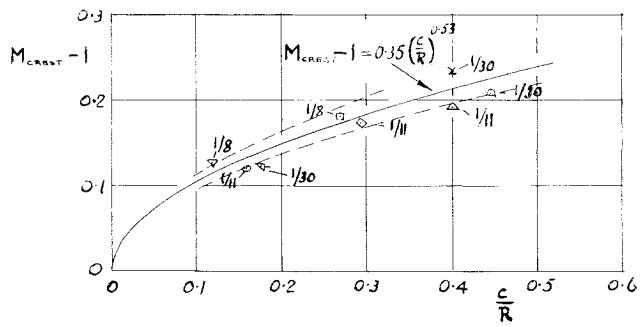

Fig. 10 Correlation of crest Mach number in a sonic stream (symbol code in Table 1).

** For a family of aerofoils varying only in thickness, $c/R \propto t/c$.

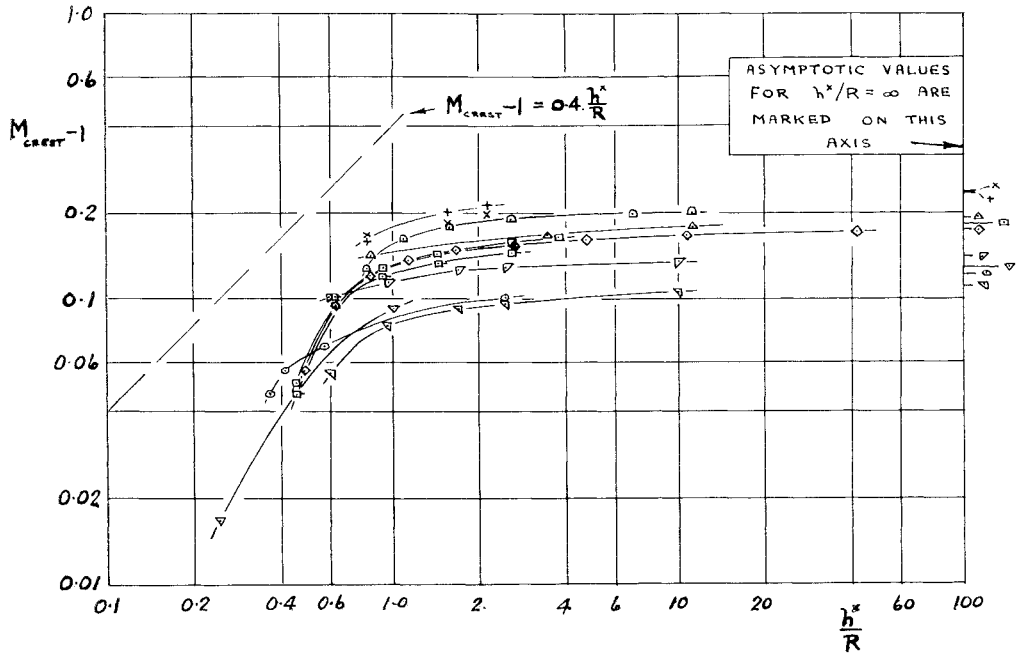

Fig. 11 Crest Mach number variation (symbol code in Table 1).

appearance of a shock wave and corresponds more closely in nature to the foregoing Eq. 7.

The left-hand portion of the curves is of the form $(M_{crest} - 1) = f(h^x/R)$ as predicted. This is seen better in Fig. 12 where only points from the steeper portion are plotted. Correlation is quite good as the maximum scatter in M_{crest} about the curve

$$(M_{crest} - 1) = 0.2(h^x/R)^{1.675}$$

is $\pm$ 2%.

Values along the right-hand portions of the various curves in Fig. 11 are scaled to one another in proportion to the value of $(M_{crest} - 1)$ at sonic speeds. The correlation obtained is shown in Fig. 13 where it is seen to be good except, of course, towards the left-hand end where the correlation of Fig. 12 applies.

2.6. Slope of Mach Number Distribution at the Crest—Sonic Speed

The chordwise slope of the Mach number distribution at the crest is found to vary very little between the critical Mach number and sonic speed. As with the crest Mach number, at sonic speed the aerofoil thickness was a variable that had no apparent effect upon the Mach number slope. Again, the prime variable was c/R; but, as might be expected with a higher order characteristic, a higher order term seemed to have an effect. As in the case of the critical Mach number this would be d^3y/dx^3, but again this was replaced by x_{crest}/c.

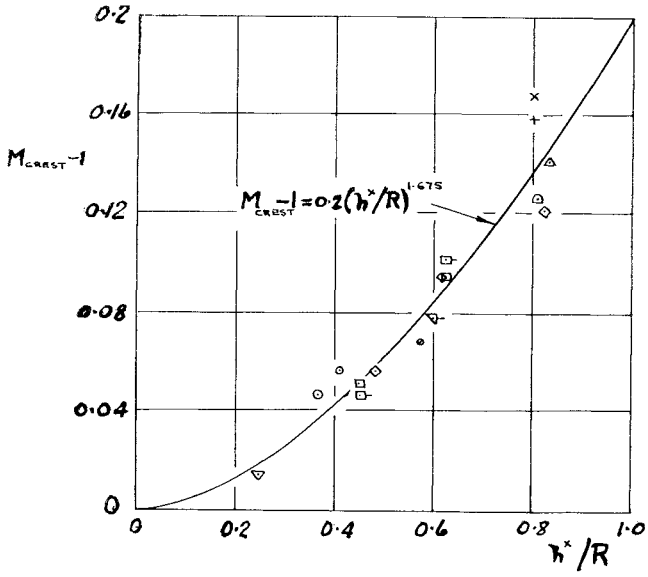

Fig. 12 Correlation of crest Mach number in the initial region (symbol code in Table 1).

The correlation obtained is shown in Fig. 14. A poor result was obtained for the 10% RAE 102 aerofoil. The experimental velocity distribution on this aerofoil was notable for having a very pronounced wave at the crest when the speed there was in the sonic region. This had a very large effect upon the velocity gradient at this speed. For some reason not apparent the results for the NACA 00095 aerofoil were unsatisfactory, the model tests giving greatly differing values for the upper and lower surfaces. With these exceptions the maximum scatter is about $\pm$4% about the curve,

$$\frac{dM/d(x/c)}{1 - 1.4[(x_{crest}/c) - 0.5]} = 4.1\left(\frac{c}{R}\right)^{1.42}$$

3. Blockage Effects

The present correlations cannot on their own justify a statement as to the absence of blockage effects. Further evidence such as that of Ref. 2 already mentioned is required for this purpose

The reason for this is that the blockage, as a correction to the aerodynamic characteristics, is a function of both the slotted working section shape and of the aerofoil shape. Or,

$$\text{blockage} = \text{f[(aerofoil), (test section)]}$$

Even if the second variable has no effect, then

$$\text{blockage} = \text{f(aerofoil)}$$

and as the true aerodynamic characteristics of the aerofoil are also a function of the shape then the measured characteristics are

$$\text{measured characteristics} = \text{true characteristics} + \text{blockage} = \text{f(aerofoil)}$$

Thus, where the measured characteristics have been expressed only as a function of the aerofoil shape, the blockage cannot be assumed consequently zero purely on the strength of these results.

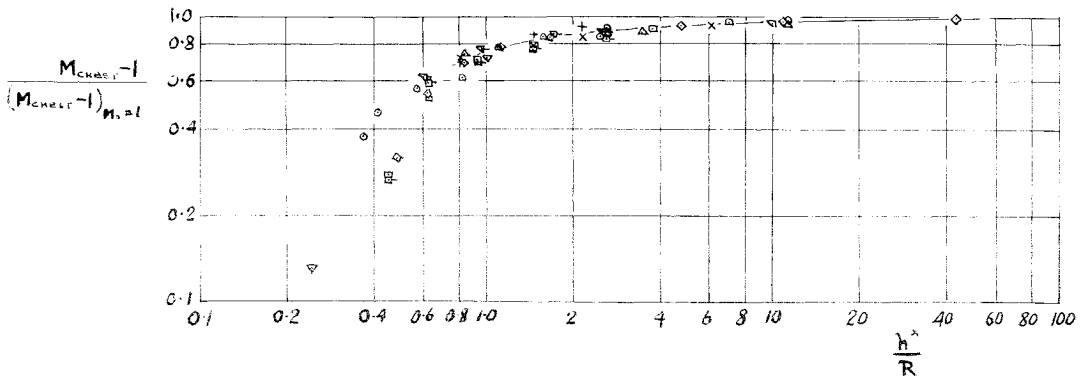

Fig. 13 Correlation of crest Mach number in the "sonic freeze" region (symbol code in Table 1).

4. Boundary-Layer Effects

Scale effects cannot be determined from the present results because all the aerofoils were tested at one and the same Reynolds number at each Mach number. The effects of the boundary layer can be estimated as follows.

The aerofoil thickness is increased by $2\delta^*$ where δ^* is the boundary-layer displacement thickness at the crest. Using primes to denote corrected shapes,

$$t'/c = (t/c) + 2(x/c)(\delta^*/x)$$

For these tests, δ^*/x was calculated to be of the order of 0.003, and as t/c varied from 0.04 to 0.10, then with $x/c = 0.4$ the correction is from 2.5 to 6%.

At the crest

$$1/R' = d^2y'/dx^2$$
$$= d^2y/dx^2 + d^2\delta^*/dx^2$$

Thus,

$$c/R' = c/R + c(d^2\delta^*/dx^2)$$

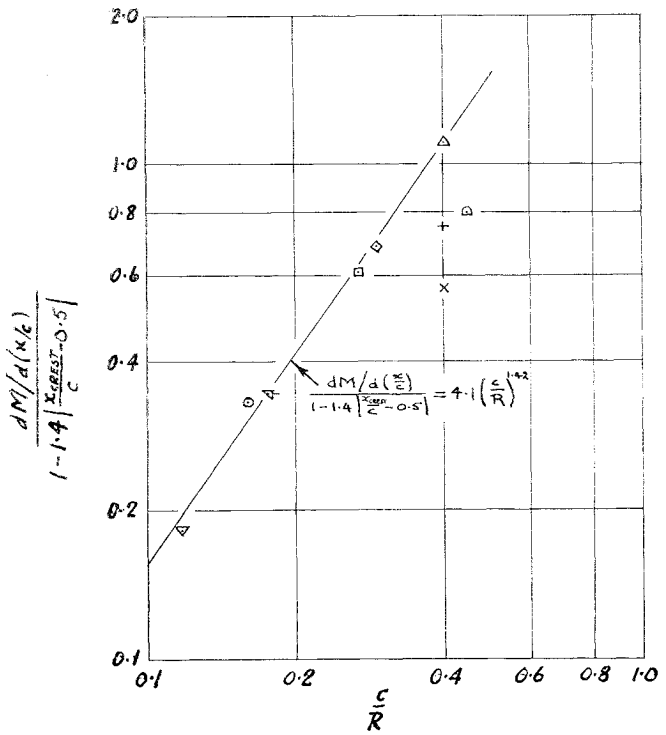

Fig. 14 Correlation of chordwise slope of the Mach number distribution in a sonic stream (symbol code in Table 1).

The value of $cd^2\delta^*/dx^2$ is -0.0012, and as c/R varied from 0.1 to 0.5 its correction rose from -0.25 to -1.2%.

Similarly,

$$\frac{t'}{R'} = \frac{t'}{c}\frac{c}{R'} = \left(\frac{t}{c} + 2\frac{x}{c}\frac{\delta^*}{x}\right)\left(\frac{c}{R} + c\frac{d^2\delta^*}{dx^2}\right)$$
$$= \frac{t}{R} + 2\frac{x}{c}\frac{\delta^*}{x}\frac{c}{R} + c\frac{d^2\delta^*}{dx^2}\frac{t}{c}$$
$$= \frac{t}{R}\left[1 + 2\frac{x}{c}\frac{\delta^*}{x}\frac{c}{t} + c\frac{d^2\delta^*}{dx^2}\frac{R}{c}\right]$$

The correction then varied from 0.021 to 0.048, that is from 2.1 to 4.8%.

5. Conclusions

The quality of the various correlations obtained suggest that the radius of curvature at the crest of an aerofoil has a strong effect upon its aerodynamic characteristics. The effect of aerofoil thickness was apparent only at the lower end of the transonic speed range.

Because the quantity of data that was used was small, one would hesitate to extrapolate the correlations obtained beyond the experimental limits even when linear relationships were obtained.

References

[1] Taylor, G. I., "The flow of air at high speed past curved surfaces," *Aeronautical Research Council* R&M 1381 (January 1930).

[2] Pearcey, H. H., Sinnett, C. S., and Osborne, J., "Some effects of wind tunnel interference observed in tests on two dimensional aerofoils at high subsonic and transonic speeds," National Physical Lab./Aero/373 (1959).

[3] Kuo, Y. H. and Sears, W. R., *General Theory of High Speed Aerodynamics* (Princeton University Press, Princeton, N. J., 1954), Vol. 6, Sec. F.

[4] Michel, R. and Sirieix, M., "Repartitions experimentales du nombre de Mach local pour differents profils d'ailes en ecoulement sonique," Office Nationale d'Etudes et de Recherches Aeronautiques Memo. Technique 17 (1959).

[5] Emmons, H. W., "The theoretical flow of a frictionless adiabatic perfect gas inside of a two dimensional hyperbolic nozzle," NACA TN 1003 (1946).

[6] Tamaki, F., "Experimental studies on the stability of the transonic flow past airfoils," *Proceedings of IXth International Congress of Applied Mechanics* (Elsevier, Amsterdam, 1957), Vol. II.

[7] Shapiro, A. H., *The Dynamics and Thermodynamics of Compressible Fluid Flow* (Ronald Press Company, New York, 1954) Vol. 2, Sec. 21.4.

[8] Gibbings, J. C., "Note on the sonic freeze concept," J. Aeroaspce Sci. **27**, 874 (1960).